Painlevé Transcendents and $\mathcal{PT}$-Symmetric Hamiltonians

Carl M. Bender^{a,b*} and Javad Komijani^{a†}

^{a}*Department of Physics, Washington University, St. Louis, MO 63130, USA*
^{b}*Department of Mathematical Science, City University London,*
Northampton Square, London EC1V 0HB, UK
(Dated: February 16, 2015)

Unstable separatrix solutions for the first and second Painlevé transcendents are studied both numerically and analytically. For a fixed initial condition, say $y(0) = 0$, there is a discrete set of initial slopes $y'(0) = b_n$ that give rise to separatrix solutions. Similarly, for a fixed initial slope, say $y'(0) = 0$, there is a discrete set of initial values $y(0) = c_n$ that give rise to separatrix solutions. For Painlevé I the large-n asymptotic behavior of b_n is $b_n \sim B_\mathrm{I} n^{3/5}$ and that of c_n is $c_n \sim C_\mathrm{I} n^{2/5}$, and for Painlevé II the large-n asymptotic behavior of b_n is $b_n \sim B_\mathrm{II} n^{2/3}$ and that of c_n is $c_n \sim C_\mathrm{II} n^{1/3}$. The constants B_I, C_I, B_II, and C_II are first determined numerically. Then, they are found analytically and in closed form by reducing the nonlinear equations to the linear eigenvalue problems associated with the cubic and quartic $\mathcal{PT}$-symmetric Hamiltonians $H = \frac{1}{2}p^2 + 2ix^3$ and $H = \frac{1}{2}p^2 - \frac{1}{2}x^4$.

I. INTRODUCTION

The famous Painlevé transcendents are six nonlinear second-order differential equations whose key features are that their movable (spontaneous) singularities are poles (and not, for example, branch points or essential singularities). There is a vast literature on these remarkable differential equations [1–8]. These equations have arisen many times in mathematical physics; for a small sample, see Refs. [9–16]. This paper considers the first and second Painlevé transcendents, referred to here as P-I and P-II. The initial-value problem (IVP) for the P-I differential equation is

$$y''(t) = 6[y(t)]^2 + t, \qquad y(0) = c, \; y'(0) = b \tag{1}$$

and the IVP for P-II (we have set an arbitrary additive constant to 0) is

$$y''(t) = 2[y(t)]^3 + ty(t), \qquad y(0) = c, \; y'(0) = b. \tag{2}$$

Many asymptotic studies of the Painlevé transcendents have been published, but in this paper we present a simple numerical and asymptotic analysis that to our knowledge has not appeared in the literature. This analysis concerns the initial conditions that give rise to special unstable separatrix solutions of P-I and P-II. Our asymptotic analysis verifies the numerical results given in this paper for P-I and P-II as well as some preliminary numerical calculations that were presented in an earlier paper on nonlinear differential-equation eigenvalue problems [17].

The main idea, originally introduced in Ref. [17], is that a nonlinear differential equation may have a discrete set of *critical* initial conditions that give rise to unstable separatrix solutions. These discrete initial conditions can be thought of as eigenvalues and the separatrices that stem from these initial conditions can be viewed as the corresponding eigenfunctions. The objective in Ref. [17] was

---

*Electronic address: cmb@wustl.edu
†Electronic address: jkomijani@physics.wustl.edu

to find the large-n (semiclassical) asymptotic behavior of the nth eigenvalue. The general analytical approach that was proposed was to simplify the nonlinear differential problem to a linear problem that could be used to determine the leading asymptotic behavior of the eigenvalues as $n \to \infty$.

A toy model was used in Ref. [17] to explain the concept of a nonlinear eigenvalue problem. This model makes use of the elementary first-order differential equation problem

$$y'(t) = \cos[\pi t \, y(t)], \quad y(0) = a. \tag{3}$$

It was shown that the solutions to this initial-value problem pass through n maxima before vanishing like $1/t$ as $t \to \infty$. As the initial condition $a = y(0)$ increases past special critical values a_n, the number of maxima jumps from n to $n + 1$. At these critical values the solution $y(t)$ to (3) is an unstable separatrix curve in the following sense: At values of $y(0)$ infinitesimally below a_n the solution merges with a bundle of stable solutions all having n maxima and when $y(0)$ is infinitesimally above a_n the solution merges with a bundle of stable solutions all having $n + 1$ maxima. The challenge is to determine the asymptotic behavior of the critical values a_n for large n. (This generic problem is the analog of a semiclassical high-energy approximation in quantum mechanics.) To solve this problem it was shown that for large n, the nonlinear differential equation problem (3) reduces to a *linear* one-dimensional random-walk problem. The random-walk problem was solved exactly, and it was shown analytically that

$$a_n \sim 2^{5/6}\sqrt{n} \quad (n \to \infty). \tag{4}$$

Kerr subsequently found an alternative solution to this asymptotics problem and verified (4) [18].

The nonlinear eigenvalue problem described above is similar in many respects to the linear eigenvalue problem for the time-independent Schrödinger equation. For a potential $V(x)$ that rises as $x \to \pm\infty$, the eigenfunctions $\psi(x)$ of the Schrödinger eigenvalue problem

$$-\psi''(x) + V(x)\psi(x) = E\psi(x), \quad \psi(\pm\infty) = 0, \tag{5}$$

are unstable with respect to small changes in the eigenvalue E; that is, if E is increased or decreased slightly, $\psi(x)$ abruptly ceases to obey the boundary conditions [and thus is not normalizable (square integrable)]. Furthermore, like the eigenfunctions (separatrix curves) of (3), the eigenfunction $\psi_n(x)$ corresponding to the nth eigenvalue has n oscillations in the classically allowed region before decreasing monotonically to 0 in the classically forbidden region.

This paper considers four eigenvalue problems. First, for P-I we find the large-n behavior of the positive eigenvalues b_n for the initial condition $y(0) = 0$, $y'(0) = b_n$ and also the large-n behavior of the negative eigenvalues c_n for the initial condition $y(0) = c_n$, $y'(0) = 0$. We show that

$$b_n \sim B_{\mathrm{I}} n^{3/5} \quad \text{and} \quad c_n \sim C_{\mathrm{I}} n^{2/5}.$$

Second, for P-II we show that for large n the asymptotic behaviors of b_n and c_n are given by

$$b_n \sim B_{\mathrm{II}} n^{2/3} \quad \text{and} \quad c_n \sim C_{\mathrm{II}} n^{1/3}.$$

We determine the constants B_{I}, C_{I}, B_{II}, and C_{II} both numerically and analytically.

This paper is organized as follows. In Sec. II we obtain the constants B_{I} and C_{I} by using numerical techniques and in Sec. III we do so analytically by reducing the large-eigenvalue problem to the *linear* time-independent Schrödinger equation for the cubic $\mathcal{PT}$-symmetric Hamiltonian $H = \frac{1}{2}p^2 + ix^3$. Next, we study the eigenvalue problem for the second Painlevé transcendent. In Sec. IV we present a numerical determination of the large-n behavior of the eigenvalues and in Sec. V we verify the numerical results in Sec. IV by using asymptotic analysis to reduce the nonlinear large-eigenvalue problem for P-II to the linear Schrödinger equation for the quartic $\mathcal{PT}$-symmetric Hamiltonian $H = \frac{1}{2}p^2 - \frac{1}{2}x^4$. In Sec. VI we make some brief concluding remarks.

II. NUMERICAL ANALYSIS OF THE FIRST PAINLEVÉ TRANSCENDENT

In Ref. [17] there is a brief numerical study of the initial-value problem for the first Painlevé transcendent (1). It is easy to see that there are two possible asymptotic behaviors as $t \to -\infty$; the solutions to the P-I equation can approach either $+\sqrt{-t/6}$ or $-\sqrt{-t/6}$. An elementary asymptotic analysis shows that if the solution $y(t)$ approaches $-\sqrt{-t/6}$, the solution oscillates stably about this curve with slowly decreasing amplitude [19]. However, while the curve $+\sqrt{-t/6}$ is a possible asymptotic behavior, this behavior is *unstable* and nearby solutions tend to veer away from it. We define the eigenfunction solutions to the first Painlevé transcendent as those solutions that *do* approach $+\sqrt{-t/6}$ as $t \to -\infty$. These separatrix solutions resemble the eigenfunctions of conventional quantum mechanics in that they exhibit n oscillations before settling down to this asymptotic behavior. However, because the P-I equation is nonlinear, these oscillations are violent; the nth eigenfunction passes through $[n/2]$ double poles where it blows up before it smoothly approaches the curve $+\sqrt{-t/6}$. (The symbol $[n/2]$ means greatest integer in $n/2$.)

One can specify two different kinds of eigenvalue problems for P-I, each of which is fundamentally related to the instability of the asymptotic behavior $+\sqrt{-t/6}$. One can (i) fix the initial value $y(0)$ and look for (discrete) values of the initial slopes $y'(0) = b$ that give rise to solutions approaching $+\sqrt{-t/6}$, or else (ii) one can fix the initial slope $y'(0)$ and look for the (discrete) initial values of $y(0) = c$ that give rise to solutions approaching $+\sqrt{-t/6}$.

A. Initial-slope eigenvalues for Painlevé I

Let us examine the numerical solutions to the initial-value problem for the P-I equation (1) for $t < 0$. To find these solutions we use Runge-Kutta to integrate down the negative-real axis. When we approach a double pole and the solution becomes large and positive, we estimate the location of the pole and integrate along a semicircle in the complex-t plane around the pole. We then continue integrating down the negative-real axis. We choose the fixed initial value $y(0) = 0$ and allow the initial slope $y'(0) = b$ to have increasingly positive values. (We only present results for positive initial slope; the behavior for negative initial slope is analogous and describing it would be repetitive.) Our numerical analysis shows that the particular choice of $y(0)$ is not crucial; for *any* fixed $y(0)$ the large-n asymptotic behavior of the initial-slope eigenvalues b_n is the same.

We find that above the critical value $b_1 = 1.851854034$ (the first eigenvalue) there is a continuous interval of b for which $y(t)$ first has a minimum and then has an infinite sequence of double poles (see Fig. 1, left panel). However, if b increases past the next critical value $b_2 = 3.004031103$ (the second eigenvalue), the character of the solutions changes abruptly and $y(t)$ oscillates stably about $-\sqrt{-t/6}$ (Fig. 1, right panel). When b exceeds the critical value $b_3 = 3.905175320$ (the third eigenvalue), the solutions again exhibit an infinite sequence of poles (Fig. 2, left panel). When b increases past the fourth critical value $b_4 = 4.683412410$ (fourth eigenvalue), the solutions once again oscillate stably about $-\sqrt{-t/6}$ (Fig. 2, right panel). Our numerical analysis indicates that there is an infinite sequence of critical points (eigenvalues) at which the P-I solutions alternate between infinite sequences of double poles and stable oscillation about $-\sqrt{-t/6}$.

The solutions that arise when $y'(0)$ is at an eigenvalue have a completely different (and unstable) character from those in Figs. 1 and 2. These special solutions pass through a *finite* number of double poles (analogous to the oscillatory behavior of quantum-mechanical bound-state eigenfunctions in the classically allowed region of a potential well) and then undergo a turning-point-like transition in which the poles cease and $y(t)$ exponentially approaches the limiting curve $+\sqrt{-t/6}$. The solutions arising from the first and second critical points b_1 and b_2 are shown in Fig. 3, those arising from the third and fourth critical points b_3 and b_4 are shown in Fig. 4, and those arising
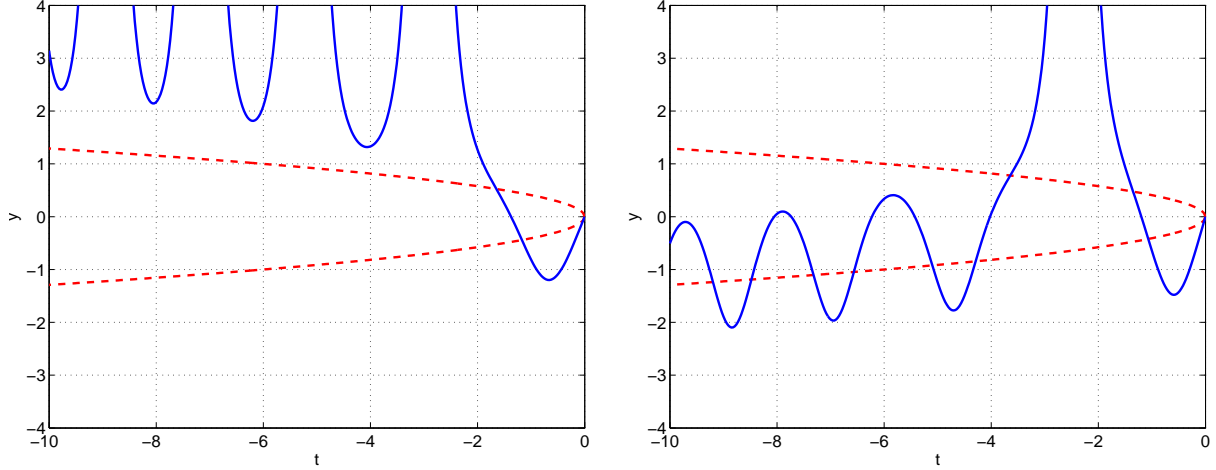
FIG. 1: Typical behavior of solutions to the first Painlevé transcendent $y(t)$ for the initial conditions $y(0) = 0$ and $b = y'(0)$. In the left panel $b = 2.504031103$, which lies between the eigenvalues $b_1 = 1.851854034$ and $b_2 = 3.004031103$. In the right panel $b = 3.504031103$, which lies between the eigenvalues $b_2 = 3.004031103$ and $b_3 = 3.905175320$. The dashed curves are $y = \pm\sqrt{-t/6}$. In the left panel the solution $y(t)$ has an infinite sequence of double poles and in the right panel the solution oscillates stably about $-\sqrt{t/6}$.

FIG. 2: Solutions to the P-I equation (1) for $y(0) = 0$ and $b = y'(0)$. Left panel: $b = 4.583412410$, which lies between the eigenvalues $b_3 = 3.905175320$ and $b_4 = 4.6834124103$. Right panel: $b = 4.783412410$, which lies between the eigenvalues $b_4 = 4.683412410$ and $b_5 = 5.383086722$.

from the tenth and eleventh critical points b_{10} and b_{11} are shown in Fig. 5. The critical points are analogous to eigenvalues because they give rise to *unstable* separatrix solutions; if $y'(0)$ changes by an infinitesimal amount above or below a critical value, the character of the solutions changes abruptly and the solutions exhibit the two possible generic behaviors shown in Figs. 1 and 2.

In Ref. [17] a numerical asymptotic study of the critical values b_n for $n \gg 1$ was performed by using Richardson extrapolation [20]. [In Ref. [17] the initial value was chosen to be $y(0) = 1$ rather than $y(0) = 0$ as in the current paper. However, as emphasized above, if $y(0)$ is held fixed, we find that the large-n asymptotic behavior of the initial slope b_n is insensitive to the choice of $y(0)$.] It was found in Ref. [17] that for large n, the nth critical value had the asymptotic behavior

$$y'_n(0) = b_n \sim B_{\mathrm{I}} n^{3/5} \quad (n \to \infty). \tag{6}$$

In Ref. [17] the constant B_{I} was determined numerically to an accuracy of about four or five decimal
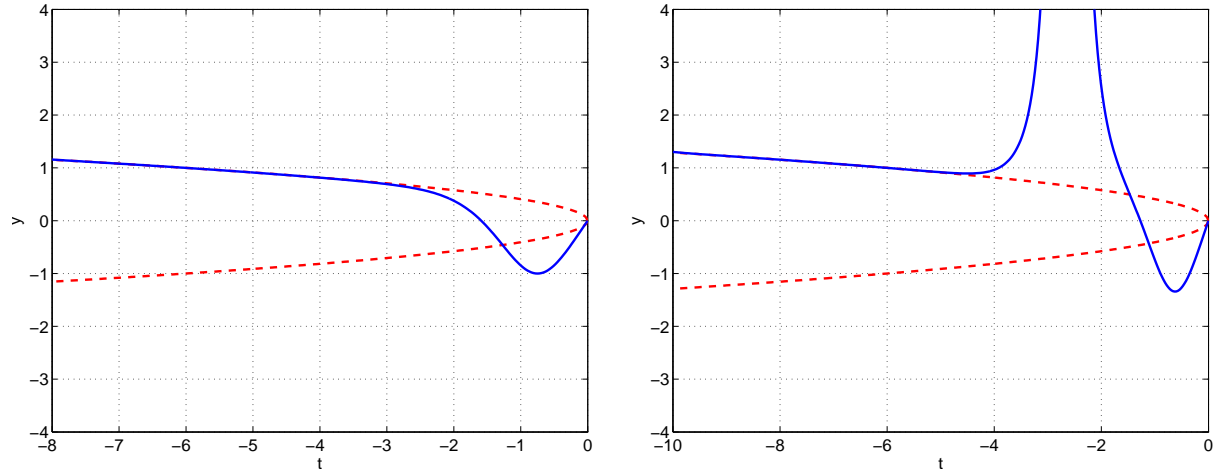
FIG. 3: First two separatrix solutions (eigenfunctions) of Painlevé I with initial condition $y(0) = 0$. Left panel: $y'(0) = b_1 = 1.851854034$; right panel: $y'(0) = b_2 = 3.004031103$. The dashed curves are $y = \pm\sqrt{-t/6}$.
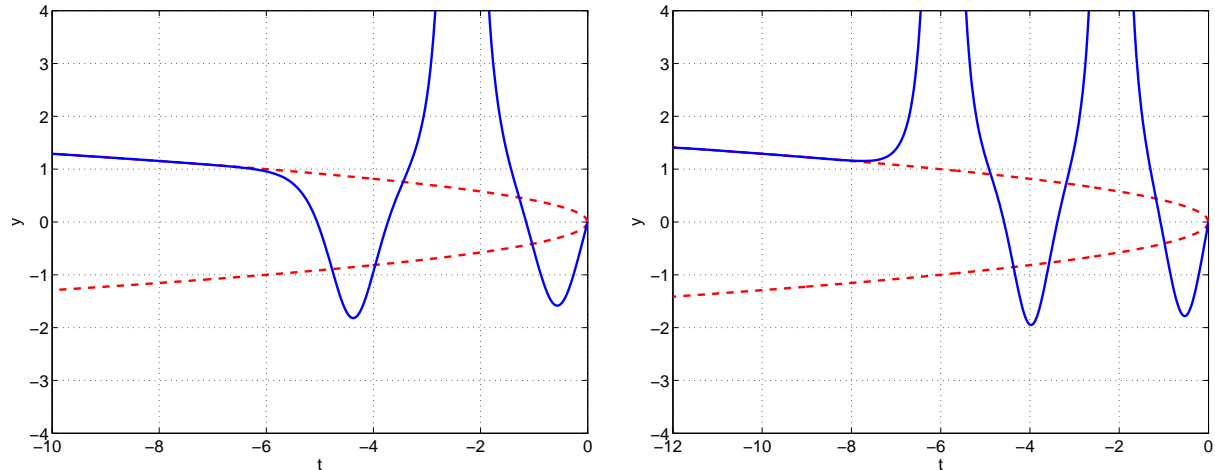

FIG. 4: Third and fourth eigenfunctions of Painlevé I with initial condition $y(0) = 0$. Left panel: $y'(0) = b_3 = 3.905175320$; right panel: $y'(0) = b_4 = 4.683412410$.

places. However, we have now performed a more accurate numerical determination of the constant B_I by applying fifth-order Richardson extrapolation to the first eleven eigenvalues, and we have found the value of B_I accurate to one part in nine decimal places:

$$B_I = 2.09214674. \tag{7}$$

On the basis of our numerical analysis, we can say with confidence that the underlined digit lies in the range from 3 to 5, so our determination of B_I is accurate to one part in 2×10^8.

B. Initial-value eigenvalues for Painlevé I

If we hold the initial slope fixed at $y'(0) = 0$ and allow the initial value $y(0) = c$ to become increasingly negative, we find that there is a sequence of negative eigenvalues c_n for which the solutions behave like the eigenfunction separatrix solutions in Figs. 3–5. The first four eigenfunctions are plotted in Figs. 6 and 7.
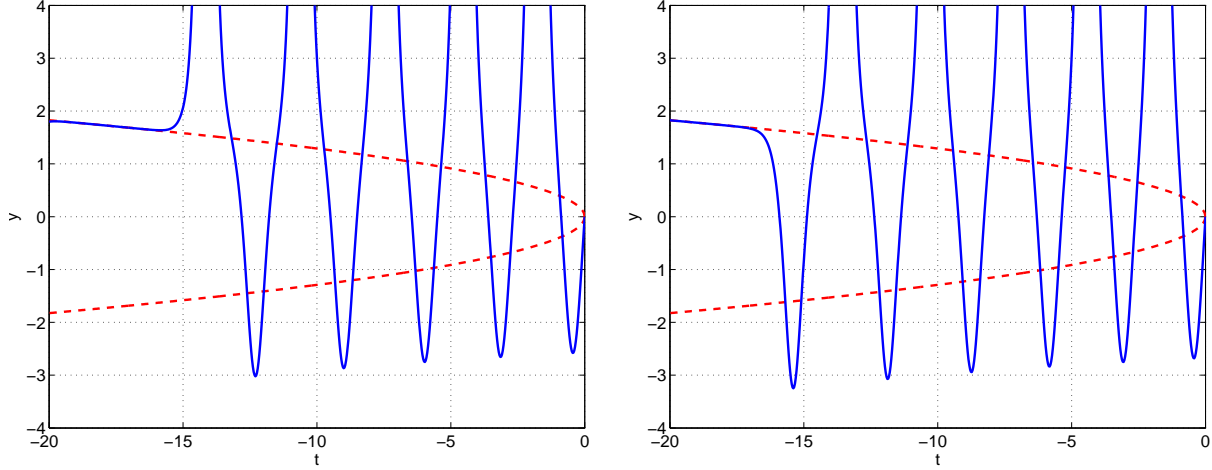
FIG. 5: Tenth and eleventh eigenfunctions of Painlevé I with initial condition $y(0) = 0$. Left panel: $y'(0) = b_{10} = 8.244932302$; right panel: $y'(0) = b_{11} = 8.738330156$. Note that as n increases, the eigenfunctions pass through more and more double poles before exhibiting a turning-point-like transition and approaching the limiting curve $+\sqrt{-t/6}$ exponentially rapidly. This behavior is analogous to that of the eigenfunctions of a time-independent Schrödinger equation for a particle in a potential well; the higher-energy eigenfunctions exhibit more and more oscillations in the classically allowed region before entering the classically forbidden region, where they decay exponentially.
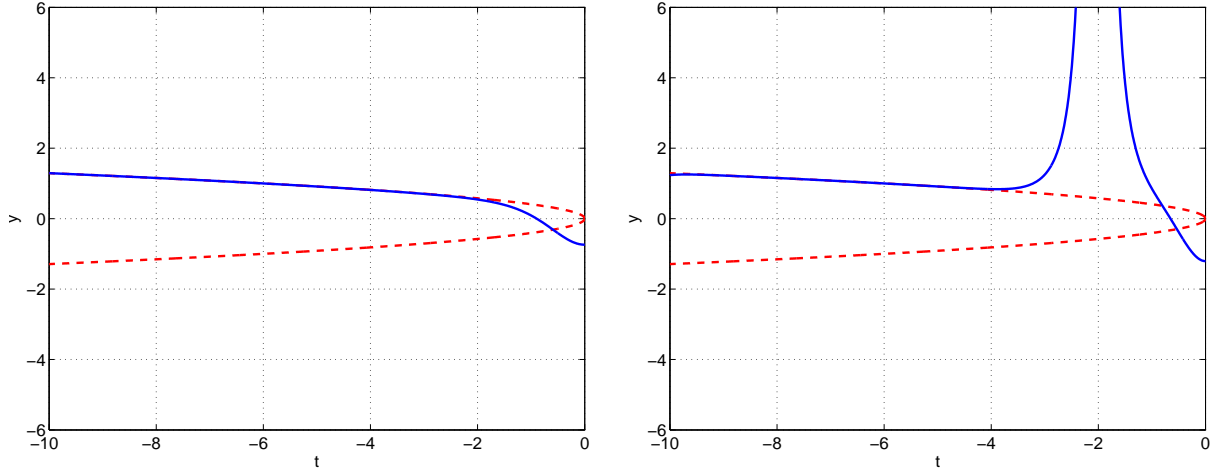

FIG. 6: First two separatrix solutions (eigenfunctions) of Painlevé I with fixed initial slope $y'(0) = 0$. Left panel: $y(0) = c_1 = -0.7401954236$; right panel: $y(0) = c_2 = -1.206703845$. The dashed curves are $y = \pm\sqrt{-t/6}$.

Applying fourth-order Richardson extrapolation to the first 15 eigenvalues, we find that for large n the sequence of initial-value eigenvalues c_n is asymptotic to $C_{\mathrm{I}} n^{2/5}$, where the numerical value of the constant C_{I} is

$$C_{\mathrm{I}} = -1.030484\underline{4}. \tag{8}$$

We are confident that the final digit is accurate to an error of ± 1 and thus C_{I} is determined to an accuracy of one part in 10^7.
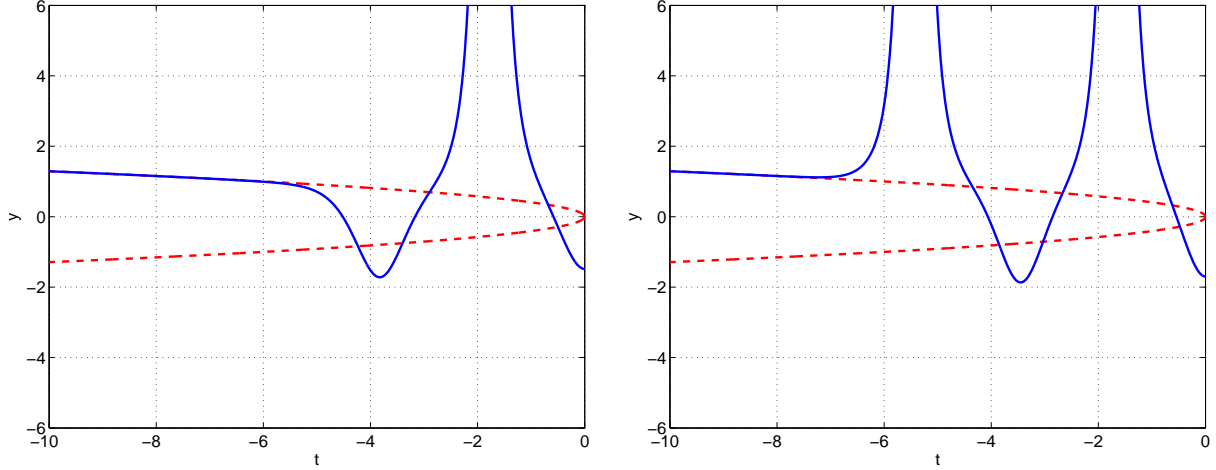
FIG. 7: Third and fourth eigenfunctions of Painlevé I with initial slope $y'(0) = 0$. Left panel: $y(0) = c_3 = -1.484375587$; right panel: $y(0) = c_4 = -1.69951765$.

III.   ASYMPTOTIC CALCULATION OF $B_{\rm I}$ AND $C_{\rm I}$

In this section we present an analytic calculation of $B_{\rm I}$ and $C_{\rm I}$ in (7) and (8). To begin, we multiply the P-I differential equation in (1) by $y'(t)$ and integrate from $t = 0$ to $t = x$. We get

$$H \equiv \tfrac{1}{2}[y'(x)]^2 - 2[y(x)]^3 = \tfrac{1}{2}[y'(0)]^2 - 2[y(0)]^3 + I(x), \tag{9}$$

where $I(x) = \int_0^x dt\, t y'(t)$. Note that the path of integration is the same as that used to calculate $y(t)$ numerically in Sec. II; it follows the negative-real axis until is gets near a pole, at which point it makes a semicircular detour in the complex-t plane to avoid the pole.

If we evaluate $I(x)$ for large $|x|$ in the classically allowed region (just before the poles abruptly cease at the turning point), we find that as $n \to \infty$, $I(x)$ fluctuates and becomes small compared with H. This is not surprising because $I(x)$ receives many positive and negative contributions from the poles. [In fact, by calculating $I(x)$ as $x \to -\infty$, we can see a clear signal of an eigenvalue; as $y'(0) = b$ passes an eigenvalue, $I(x)$ goes from having positive to negative (or negative to positive) fluctuations but at an eigenvalue $I(x)$ is smooth and not fluctuating.] Thus, for large n we treat the fluctuating quantity $I(x)$ as small, and if we do so we can interpret H as a time-independent quantum-mechanical Hamiltonian. [The isomonodromic properties of H when $I(x)$ is not neglected were studied in Ref. [6].]

We conclude that the large-n (semiclassical) behavior of the eigenvalues [that is, the initial conditions in (1)] can be determined by solving the *linear* quantum-mechanical eigenvalue problem $\hat{H}\psi = E\psi$, where $\hat{H} = \tfrac{1}{2}\hat{p}^2 - 2\hat{x}^3$. To find these eigenvalues we rotate $\hat{H}$ into the complex plane [21] and obtain the well-studied $\mathcal{PT}$-symmetric Hamiltonian [22]

$$\hat{H} = \tfrac{1}{2}\hat{p}^2 + 2i\hat{x}^3. \tag{10}$$

The large eigenvalues of this Hamiltonian can be found by using the complex WKB techniques discussed in detail in Ref. [22]. For the general class of $\mathcal{PT}$-symmetric Hamiltonians $\hat{H} = \tfrac{1}{2}\hat{p}^2 + g\hat{x}^2 (i\hat{x})^\epsilon$ ($\epsilon \geq 0$), the WKB approximation to the nth eigenvalue ($n \gg 1$) is given by

$$E_n \sim \frac{1}{2}(2g)^{2/(4+\epsilon)} \left[\frac{\Gamma\left(\frac{3}{2} + \frac{1}{\epsilon+2}\right)\sqrt{\pi}\, n}{\sin\left(\frac{\pi}{\epsilon+2}\right)\Gamma\left(1 + \frac{1}{\epsilon+2}\right)} \right]^{(2\epsilon+4)/(\epsilon+4)}. \tag{11}$$

Thus, for H in (10) we take $g = 2$ and $\epsilon = 1$ and obtain the asymptotic behavior

$$E_n \sim 2 \left[\sqrt{3\pi} \Gamma \left(\tfrac{11}{6} \right) n / \Gamma \left(\tfrac{1}{3} \right) \right]^{6/5} \quad (n \to \infty). \tag{12}$$

Since $\hat{H}$ in (10) is time independent, we can evaluate H in (9) for fixed $y(0)$ and large $y'(0) = b_n$ and obtain the result that

$$b_n \sim \sqrt{2E_n} = B_{\mathrm{I}} n^{3/5} \quad (n \to \infty), \tag{13}$$

which verifies (6). We then read off the analytic value of the constant B_{I}:

$$B_{\mathrm{I}} = 2 \left[\sqrt{3\pi} \Gamma \left(\tfrac{11}{6} \right) / \Gamma \left(\tfrac{1}{3} \right) \right]^{3/5}, \tag{14}$$

which agrees with the numerical result in (7). Also, if we take the initial slope $y'(0)$ to vanish and take the initial condition $y(0) = c_n$ to be large, we obtain an analytic expression for C_{I},

$$C_{\mathrm{I}} = - \left[\sqrt{3\pi} \Gamma \left(\tfrac{11}{6} \right) / \Gamma \left(\tfrac{1}{3} \right) \right]^{2/5}, \tag{15}$$

which agrees with the numerical result in (8).

IV.   NUMERICAL ANALYSIS OF THE SECOND PAINLEVÉ TRANSCENDENT

To understand the behavior of solutions to the initial-value problem in (2) for Painlevé II, we follow the procedure used in Sec. II to study P-I. An elementary asymptotic analysis shows that as $t \to -\infty$, there are three possible asymptotic behaviors for solutions $y(t)$. First, $y(t)$ can oscillate stably about the negative axis. Second, $y(t)$ can approach the curves $\pm\sqrt{-t/2}$; however, both of these asymptotic behaviors are unstable.

If we numerically integrate (2), we observe that when t becomes large and negative, a typical solution to the P-II initial-value problem either oscillates about the negative axis or passes through an infinite sequence of simple poles. However, it is also possible to find special eigenfunction solutions that pass through only a finite number of poles and then approach either the positive or the negative branches of the square-root curves. These eigenfunctions obey the boundary conditions $y(0) = 0$ and $y'(0) = \pm b$. [Note that P-II is symmetric under $y \to -y$, so there are two sets of eigenfunctions, one for each sign of $y'(0)$.] We study these eigenfunctions numerically in Subsec. IV A. The P-II equation is particularly interesting because as $t \to +\infty$, the behavior $y \to 0$ becomes unstable. Thus, it is possible to have new kinds of eigenfunctions for positive t as well. We seek eigenfunctions that satisfy $y'(0) = 0$ and $y(0) = c$ and examine the positive-c eigenfunctions numerically in Subsec. IV B.

A.   Initial-slope eigenvalues for Painlevé I

Similar to what we found in Sec. II, if we choose $y(0) = 0$, there are critical values $y'(0) = b_n$ at which the solutions $y(t)$ change their character. In Figs. 8 and 9 we plot the solutions to the P-II equation for the initial condition $y(0) = 0$ and $y'(0) = b$ for $b_1 < b < b_2$, $b_2 < b < b_3$, $b_3 < b < b_4$, and $b_4 < b < b_5$. Note that in these figures the character of the solution alternates between having an infinite sequence of simple poles and oscillating stably about $y(t) = 0$. However, when $y'(0) = b$ is at a critical value (eigenvalue) b_n, the solution $y(t)$ passes through a *finite* number $[n/2]$ of simple
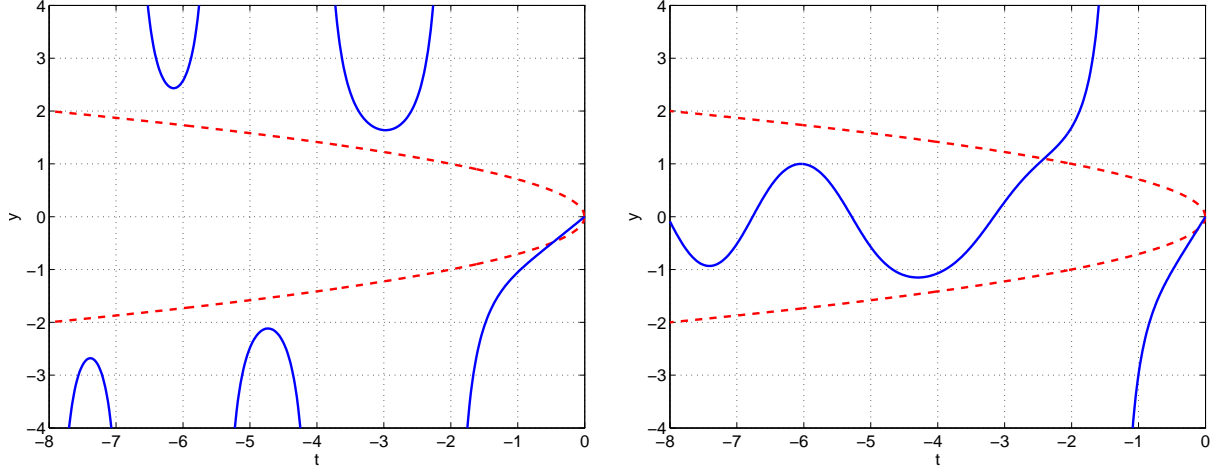
FIG. 8: Typical behavior of solutions to the second Painlevé transcendent for the initial conditions $y(0) = 0$ and $b = y'(0)$. In the left panel $b = 1.028605106$, which lies between the eigenvalues $b_1 = 0.5950825526$ and $b_2 = 1.528605106$. In the right panel $b = 2.028605106$, which lies between the eigenvalues $b_2 = 1.528605106$ and $b_3 = 2.155132869$. In the left panel the solution $y(t)$ has an infinite sequence of simple poles and in the right panel the solution oscillates stably about $-\sqrt{t/6}$. The dashed curves are the functions $\pm\sqrt{-t/2}$.
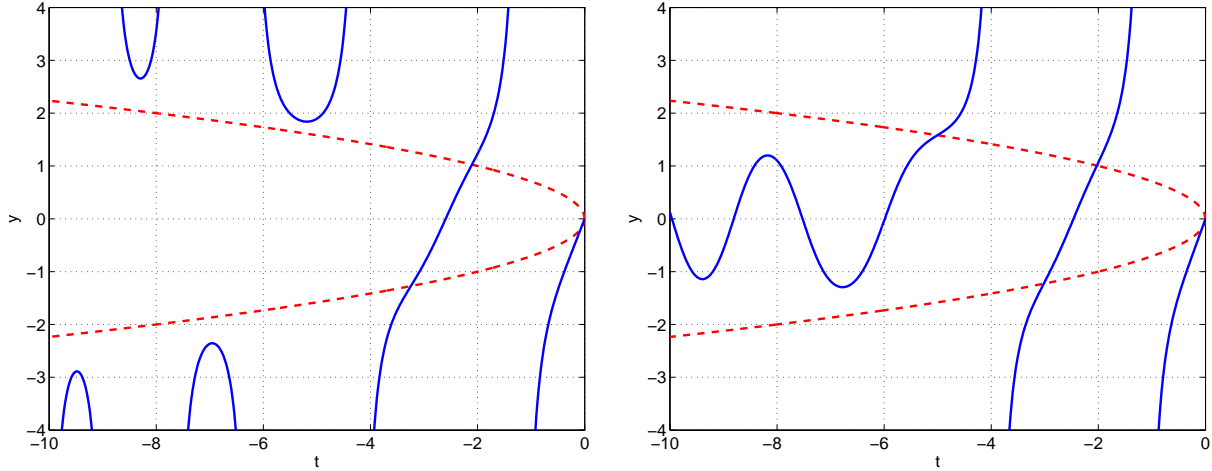

FIG. 9: Solutions to the P-II equation (2) for $y(0) = 0$ and $b = y'(0)$. Left panel: $b = 2.600745985$, which lies between the eigenvalues $b_3 = 2.155132869$ and $b_4 = 2.700745985$. Right panel: $b = 2.800745985$, which lies between the eigenvalues $b_4 = 2.700745985$ and $b_5 = 3.195127590$.

poles and then approaches either $+\sqrt{-t/2}$ or $-\sqrt{-t/2}$. These eigenfunctions (separatrices) are plotted in Figs. 10, 11, and 12 for $n = (1, 2)$, $(3, 4)$, and $(20, 21)$.

Note that the eigenfunctions in Figs. 10, 11, and 12 alternate between approaching the upper-unstable branch $+\sqrt{-t/2}$ or the lower-unstable branch $-\sqrt{-t/2}$, and thus there are actually two sequences of eigenvalues, one for even n and one for odd n. Using Richardson extrapolation, we find that the sequences of eigenvalues b_{2n} and b_{2n+1} have the same asymptotic behavior

$$b_{2n} \sim b_{2n+1} \sim B_{\text{II}} n^{2/3} \quad (n \to \infty). \tag{16}$$

Our numerical calculations give

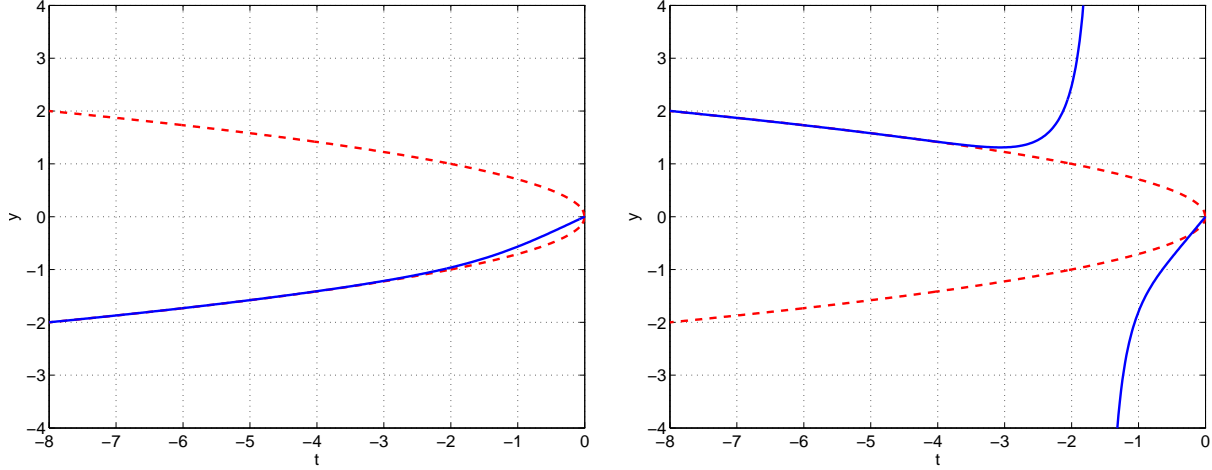$$B_{\text{II}} = 1.8624128. \tag{17}$$

FIG. 10: First two separatrix solutions (eigenfunctions) of Painlevé II with initial condition $y(0) = 0$. Left panel: $y'(0) = b_1 = 0.5950825526$; right panel: $y'(0) = b_2 = 1.528605106$. The dashed curves are $\pm\sqrt{-t/2}$.
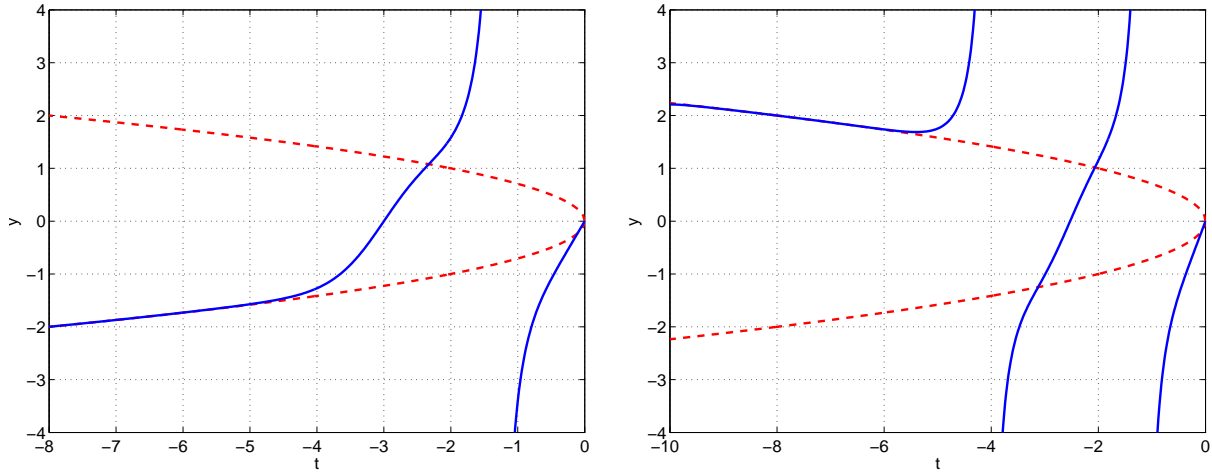

FIG. 11: Third and fourth eigenfunctions of Painlevé II with initial condition $y(0) = 0$. Left panel: $y'(0) = b_3 = 2.155132869$; right panel: $y'(0) = b_4 = 2.700745985$.

The numerical data for P-II are slightly more noisy than those for P-I, and fourth-order Richardson extrapolation only gives the underlined eighth digit as 8 ± 2.

B. Initial-value eigenvalues for Painlevé II

Next, we plot the positive-t solutions to P-II for vanishing initial slope and positive initial condition for $t \geq 0$. As $t \to \infty$, the nth eigenfunction passes through n simple poles before it approaches zero monotonically. In Figs. 13, 14, and 15 we plot the six eigenfunctions corresponding to $n = (1, 2)$, $(3, 4)$, and $(13, 14)$. (Because of the symmetry of P-II, for every positive eigenvalue there is a corresponding negative eigenvalue. We do not plot the negative-eigenvalue solutions.)

Using fourth-order Richardson we determine that for large n, $c_n \sim C_{\mathrm{II}} n^{1/3}$, where

$$C_{\mathrm{II}} = 1.2158116\underline{5}. \tag{18}$$

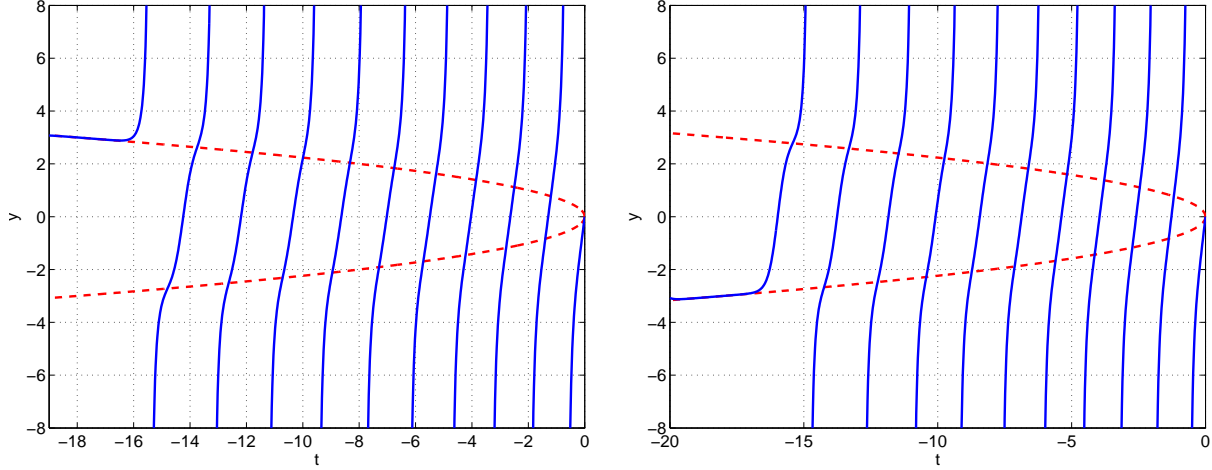The last digit 5 has an uncertainty of ± 1.

FIG. 12: The twentieth and twenty-first eigenfunctions of Painlevé II with initial condition $y(0) = 0$. Left panel: $y'(0) = b_{20} = 8.499476190$; right panel: $y'(0) = b_{21} = 8.787666814$.
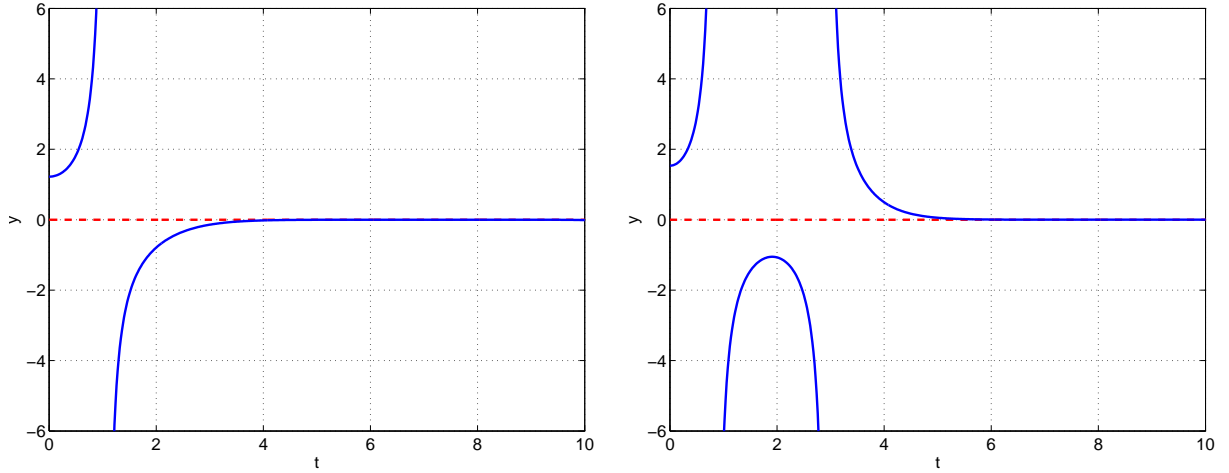

FIG. 13: First two separatrix solutions (eigenfunctions) of Painlevé II with fixed initial slope $y'(0) = 0$. Left panel: $y(0) = c_1 = 1.222873339$; right panel: $y(0) = c_2 = 1.533883935$.

V.   ASYMPTOTIC CALCULATION OF B_{II} AND C_{II}

To obtain analytic expressions for B_{II} in (17) and C_{II} in (18), we follow the same procedure as in Sec. III for P-I. We multiply the P-II differential equation in (2) by $y'(t)$ and integrate from $t = 0$ to $t = x$, where x is in the turning-point region which the simple poles stop. The result is

$$H \equiv \tfrac{1}{2}[y'(x)]^2 - \tfrac{1}{2}[y(x)]^4 = \tfrac{1}{2}[y'(0)]^2 - \tfrac{1}{2}[y(0)]^4 + I(x), \qquad (19)$$

where $I(x) = \int_0^x dt\, t y(t) y'(t)$. The path of integration is the same as that used to calculate P-II numerically in Sec. IV; it follows the negative-real axis until it gets near a simple pole, at which point it makes a semicircular detour in the complex-t plane to avoid the pole. Again, as in Sec. III, we argue that along this path the integrand of $I(x)$ is oscillatory and because of cancellations we may neglect $I(x)$ when n is large.

We treat H as the $\mathcal{PT}$-symmetric quantum-mechanical Hamiltonian

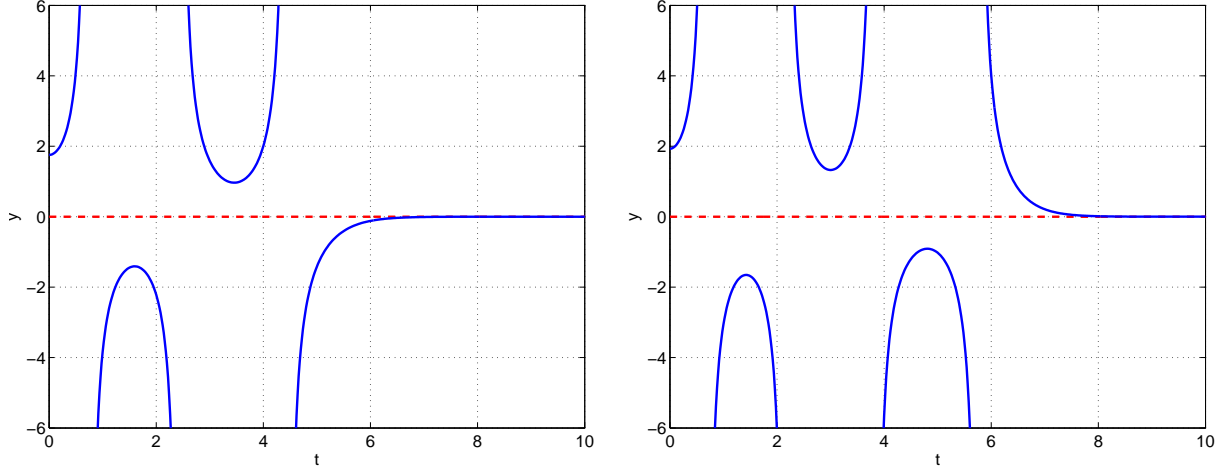$$\hat{H} = \tfrac{1}{2}\hat{p}^2 - \tfrac{1}{2}\hat{x}^4 \qquad (20)$$

FIG. 14: Third and fourth eigenfunctions of Painlevé II with initial slope $y'(0) = 0$. Left panel: $y(0) = c_3 = 1.754537281$; right panel: $y(0) = c_4 = 1.93061783$.
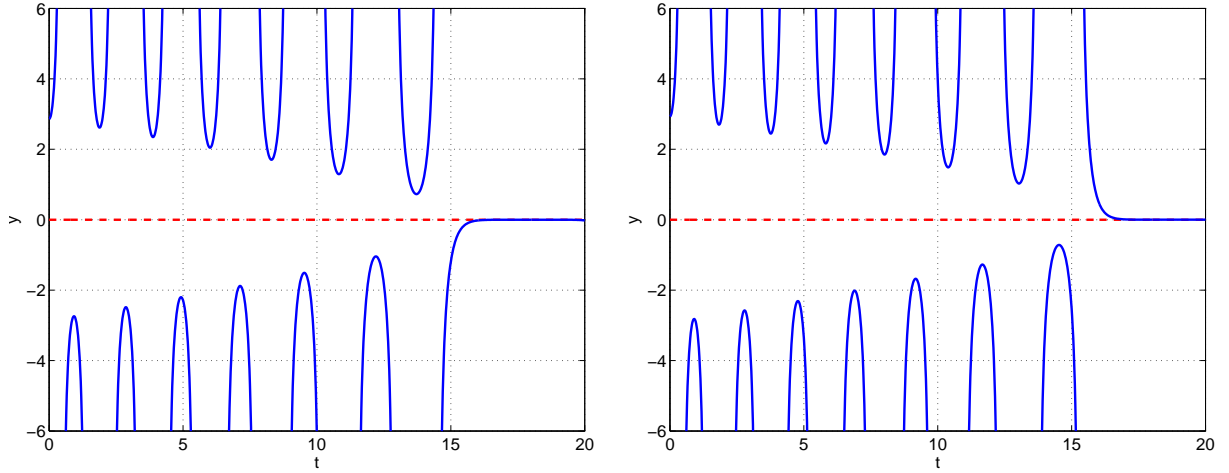

FIG. 15: Thirteenth and fourteenth separatrix solutions (eigenfunctions) of Painlevé II with fixed initial slope $y'(0) = 0$. Left panel: $y(0) = c_1 = 2.858869051$; right panel: $y(0) = c_2 = 2.9303576515$.

and we use (11) with $g = 1/2$ and $\epsilon = 2$ to obtain the formula

$$E_n \sim \tfrac{1}{2} \left[3n\sqrt{2\pi}\Gamma\left(\tfrac{3}{4}\right) / \Gamma\left(\tfrac{1}{4}\right) \right]^{4/3} \tag{21}$$

for the large eigenvalues of $\hat{H}$. Finally, we calculate the eigenvalues b_n by using

$$\sqrt{2E_n} \sim \left[3n\sqrt{2\pi}\Gamma\left(\tfrac{3}{4}\right) / \Gamma\left(\tfrac{1}{4}\right) \right]^{2/3} \quad (n \to \infty). \tag{22}$$

This result allows us to identify the value of B_{II} in (17) as

$$B_{\mathrm{II}} = \left[3\sqrt{2\pi}\Gamma\left(\tfrac{3}{4}\right) / \Gamma\left(\tfrac{1}{4}\right) \right]^{2/3}. \tag{23}$$

This result agrees with the numerical determination in (17).

To calculate C_{II} we observe from Figs. 13-15 that the initial value $y(0)$ is positive. However, if we neglext $I(x)$ and assume a vanishing initial slope, we see that the right side of (19) negative.

Thus, as we did for the cubic Hamiltonian $\frac{1}{2}\hat{p}^2 - 2\hat{x}^3$, we perform a complex rotation of the coupling constant to convert the quartic Hamiltonian to the form

$$\hat{H} = \tfrac{1}{2}\hat{p}^2 + \tfrac{1}{2}\hat{x}^4. \tag{24}$$

This is the conventional Hermitian quartic-anharmonic-oscillator Hamiltonian, and does not belong to the class of $\mathcal{PT}$-symmetric Hamiltonians $\hat{H} = \frac{1}{2}\hat{p}^2 + g\hat{x}^2(i\hat{x})^\epsilon$. A WKB calculation gives the large-eigenvalue approximation

$$E_n \sim \left[3n\sqrt{\pi}\Gamma\left(\tfrac{3}{4}\right)/\Gamma\left(\tfrac{1}{4}\right)\right]^{4/3} \quad (n \to \infty). \tag{25}$$

Thus, we read off the value of C_{II}:

$$C_{II} = \left[3\sqrt{\pi}\Gamma\left(\tfrac{3}{4}\right)/\Gamma\left(\tfrac{1}{4}\right)\right]^{1/3}, \tag{26}$$

which agrees exactly with the numerical result in (18).

VI.   BRIEF CONCLUDING REMARKS

In this paper we have shown that the first two Painlevé equations, P-I and P-II, exhibit instabilities that are associated with separatrix solutions. The initial conditions that give rise to these separatrix solutions are eigenvalues. We have calculated the semiclassical (large-eigenvalue) behavior of the eigenvalues in two ways, first by using numerical techniques and then by using asymptotic methods to reduce the initial-value problems for the nonlinear P-I and P-II equations to linear eigenvalue problems associated with the time-independent Schrödinger equation. The agreement between these two approaches is exact.

The obvious continuation of this work is to examine the next four Painlevé equations, P-III — P-VI, to see if there are instabilities, separatrices, and eigenvalues for these equations as well. However, the techniques we have applied here may also be useful for other nonlinear differential equations such as the Thomas-Fermi equation $y''(x) = [y(x)]^{3/2}/\sqrt{x}$, which is posed as a boundary-value problem satisfying the boundary conditions $y(0) = 1$ and $y(\infty) = 0$. The solution to this problem is *unstable* with respect to small changes in the initial data; if the initial slope $y'(0)$ is varied by a small amount, the solution develops a spontaneous singularity at some positive value a. A leading-order local analysis suggests that this singularity is a fourth-order pole of the form $400(x-a)^{-4}$. However, this singularity is not a pole. Indeed, a higher-order local analysis indicates that there is a logarithmic-branch-point singularity at $x = a$ as well and thus the solutions to the Thomas-Fermi equation live on multisheeted Riemann surfaces. It would be interesting to see if our work on nonlinear eigenvalue problems extends beyond meromorphic functions.

[1] E. L. Ince, *Ordinary Differential Equations* (Dover, New York, 1956).
[2] A detailed study of the asymptotic behavior of the Painlevé transcendents may be found in M. Jimbo and T. Miwa, Physica D **2**, 407 (1981).
[3] Separatrix behavior of the first Painlevé transcendent is mentioned briefly in A. A. Kapaev, Differential Equations **24**, 1107 (1989).
[4] P. A. Clarkson, J. Comp. Appl. Math. **153**, 127 (2003).
[5] D. Maseoro, *Essays on the Painlevé First Equation and the Cubic Oscillator*, PhD Thesis, SISSA (2010).
[6] T. Kawai and Y. Takei, *Algebraic Analysis of Singular Perturbation Theory*, (American Mathematical Society, New York, 2005).

[7] O. Costin, R. D. Costin, and M. Huang, *Tronquée solutions of the Painlevé equation P_1* (2013, unpublished).

[8] A. S. Fokas, A. R. Its, A. A. Kapaev, and V. Y. Novokshonov, *Painlevé Transcendents: The Riemann-Hilbert Approach*, (American Mathematical Society, New York, 2006).

[9] The spin-spin correlation function for the two-dimensional Ising model for temperatures near T_c is described by P-III. See T. T. Wu, B. M. McCoy, C. A. Tracy, and E. Barouch, Phys. Rev. B **13**, 316 (1976).

[10] For all temperatures the diagonal correlation function for the Ising model in two dimensions $\langle \sigma_{0,0} \sigma_{N,N} \rangle$ is given in terms of P-VI. See M. Jimbo and T. Miwa, Proc. Jap. Acad. **56A**, 405 (1980) and **57A**, 347 (1981).

[11] E. Brézin and V. A. Kazakov, Phys. Lett. B **236**, 144 (1990).

[12] M. Douglas and S. Shenker, Nucl. Phys. B **335**, 635 (1990).

[13] D. Gross and A. Migdal, Nucl. Phys. B **340**, 333 (1990).

[14] G. Moore, Comm. Math. Phys. **133**, 261 (1990).

[15] G. Moore, Prog. Theor. Phys. Suppl. **102**, 255 (1990).

[16] A. S. Fokas, A. R. Its, and A. V. Kitaev, Comm. Math. Phys. **147**, 395 (1992).

[17] C. M. Bender, A. Fring, and J. Komijani, J. Phys. A: Math. Theor. **47**, 235204 (2014).

[18] O. S. Kerr, J. Phys. A: Math. Theor. **47**, 368001 (2014).

[19] C. M. Bender and S. A. Orszag, *Advanced Mathematical Methods for Scientists and Engineers* (McGraw Hill, New York, 1978), chap. 4.

[20] See Ref. [19], Chap. 8.

[21] For a discussion of complex scaling (complex rotation of coordinates) see W. P. Reinhardt, Ann. Rev. Phys. Chem. **33**, 223 (1982).

[22] C. M. Bender and S. Boettcher, Phys. Rev. Lett. **80**, 5243 5246 (1998).